Optical Modulator Optimization for Orthogonal Frequency-Division Multiplexing

Daniel J. Fernandes Barros and Joseph M. Kahn, *Fellow, IEEE*

***Abstract*—Orthogonal frequency-division multiplexing (OFDM) has a high peak-to-average ratio (PAR), which can result in low optical power efficiency when modulated through a Mach–Zehnder (MZ) modulator. In addition, the nonlinear characteristic of the MZ can cause significant distortion on the OFDM signal, leading to in-band intermodulation products between subcarriers. We show that a quadrature MZ with digital predistortion and hard clipping is able to overcome the previous impairments. We consider quantization noise and compute the minimum number of bits required in the digital-to-analog converter (D/A). Finally, we discuss a dual-drive MZ as a simpler alternative for the OFDM modulator, but our results show that it requires a higher oversampling ratio to achieve the same performance as the quadrature MZ.**

***Index Terms*—Coherent optical communications, CO-OFDM, dual-drive Mach–Zehnder (MZ) modulator, orthogonal frequency-division multiplexing (OFDM), MZ modulator, quadrature MZ modulator.**

I. Introduction

ORTHOGONAL frequency-division multiplexing (OFDM) is a multicarrier modulation that is receiving increased interest in the fiber-optic research community for its robustness against intersymbol interference (ISI), since the symbol period of each subcarrier can be made long compared to the delay spread caused by group-velocity dispersion (GVD) and polarization-mode dispersion (PMD) [1], [2].

Multicarrier signals like OFDM have a high peak-to-average ratio (PAR), which is proportional to the number of used subcarriers [3]. Optical OFDM is modulated using Mach–Zehnder (MZ) modulators having nonlinear, peak-limited transfer characteristics. Experiments have been performed demonstrating the potential of OFDM with coherent detection in optical systems [1], [4], [5]. Some previous work has investigated the possibility of predistortion and clipping to mitigate the effects of MZ nonlinearity on OFDM system performance [5], [6]. Our study extends that previous work by considering the frequency-dependent MZ electrode losses, by quantifying optical power efficiency, and by introducing the dual-drive MZ as an alternative option for the OFDM modulator.

There are several options to generate an optical OFDM signal. A popular technique shifts the electrical OFDM signal to an intermediate frequency (IF) and then uses it to drive a single MZ modulator [1], [4], [5]. Another option is to use a quadrature MZ. A quadrature MZ modulates directly the baseband electrical OFDM signal to the optical domain without the need of an IF. Hence, this technique, sometimes called direct conversion [5], reduces the required electrical bandwidth by a factor of two, at the expense of a more complicated modulator design. A conventional solution to the PAR problem is to reduce the operating range in the MZ to accommodate the OFDM peak. However, this solution results in a significant power efficiency penalty, which may require the use of optical amplification at the transmitter to boost the signal level. An alternative solution would be using peak-reduction algorithms studied for wireless systems [3]. All of these peak-reduction algorithms, however, lead to undesired effects, such as increased coding overhead and/or increased average transmitted power [7]–[10]. An increased coding overhead requires an increased sampling rate in order to maintain the desired bit rate, exacerbating the impact of GVD and PMD, and requiring faster digital-to-analog (D/A) converters. An increased average transmitted power can lead to increased nonlinear impairment; in [11], it was shown that the variance of phase noise caused by four-wave mixing is proportional to the power in each subcarrier, but is not simply related to the instantaneous peak power. Furthermore, all of the peak-reduction algorithms present a computational burden to the transmitter [10], which might be prohibitive at the speeds of optical systems.

In this paper, we present hard clipping with predistortion as a simple and effective approach to combat the nonlinearity in the quadrature MZ and increase the optical power efficiency. Since the OFDM peaks occur with a very low probability, clipping can be an effective technique. In addition, we study the combined effects of having a finite number of bits in the D/A and the MZ nonlinearity. We then extend our study to the dual-drive MZ, which proves to require a higher oversampling ratio to achieve the same performance as the quadrature MZ.

This paper is organized as follows. In Section II, we review PAR fundamentals in multicarrier systems and the quadrature drive MZ modulator. In addition, we introduce the MZ canonical model including the electrode frequency response. In Section III, we focus on the quadrature MZ, and study through simulations the optical power efficiency (OPE) and system performance gains when predistortion and hard clipping are used. Moreover, we consider quantization noise from the D/A and study through simulations the minimum number of bits required and the optimum clipping level. In Section IV, we introduce the dual-drive MZ as a simpler option for the OFDM modulator. We then analyze the oversampling required to achieve low performance degradation in the dual-drive MZ.

Manuscript received June 26, 2008; revised October 23, 2008. First published April 17, 2009; current version published June 26, 2009. This work was supported by Naval Research Laboratory Award N00173-06-1-G035, by the Portuguese Foundation for Science and Technology Scholarship SFRH/BD/22547/2005 and by a Stanford Graduate Fellowship.

The authors are with the Department of Electrical Engineering, Stanford University, Stanford, CA 94305-9515 USA (e-mail: djbarros@stanford.edu, jmk@ee.stanford.edu).

Digital Object Identifier 10.1109/JLT.2008.2010002

II. PAR AND MZ REVIEW

A. Peak-to-Average Power Ratio

The PAR is defined as [3]

$$\mathrm{PAR} = \frac{\max_t |x(t)|^2}{E\{x(t)^2\}} \tag{1}$$

where $\max_t |x(t)|^2$ is the peak value squared of the signal $x(t)$ and $E\{x(t)^2\}$ is the average signal power. The peak of the signal determines the dynamic range required of the D/As and modulators in the circuit. Thus, it is desirable to have signals with low PAR. In the case of OFDM, i.e., identical constellations on all of the subcarriers, the PAR can be written as [3], [10]

$$\mathrm{PAR} = N_u \frac{\max_k |X_k|^2}{E\{X_k)^2\}} \tag{2}$$

where $\max_k |X_k|^2$ is the largest symbol magnitude squared on the kth subcarrier, $E\{X_k)^2\}$ is the average power per symbol on subcarrier k and N_u is the number of used subcarriers. In particular, if all the subcarriers are modulated using QPSK, (2) becomes

$$\mathrm{PAR} = N_u. \tag{3}$$

B. Mach–Zehnder Modulator

If complementary drive signals are used, the transfer characteristic of a single-drive MZ modulator is [12]

$$\frac{E_{\mathrm{out}}(t)}{E_{\mathrm{in}}(t)} = \sin\left(\frac{\pi V_m(t)}{2V_\pi}\right) \tag{4}$$

where $E_{\mathrm{out}}(t)$ and $E_{\mathrm{in}}(t)$ are the output and input electric fields, respectively, $V_m(t)$ is the electrical modulator signal, and V_π is the voltage that must be applied to the single electrode to produce a differential phase shift of π between the two waveguides. The modulator electrode has frequency-dependent loss, so that high-frequency components of the drive signal are attenuated. The electrode frequency response can be modeled by [12]

$$\frac{V_m(f)}{V_d(f)} = \frac{1 - e^{-\alpha(f)L + j2\pi f d_{12} L}}{\alpha(f)L - j2\pi f d_{12} L} \tag{5}$$

where V_d is the input drive voltage, V_m is the modulating voltage of the MZ transfer characteristic, $\alpha(f)$ is the frequency-dependent loss, d_{12} is the velocity mismatch difference between the optical and electrical waveguides and L is the interaction length. The model for single-drive MZ modulator is shown in Fig. 1.

Two single-drive MZ modulators can be combined to create a quadrature MZ. The quadrature MZ comprises two single-drive MZs, whose output optical fields are added in quadrature. The quadrature MZ is useful to modulate a complex baseband signal directly to the optical domain without the need of shifting the signal to an IF. Fig. 2 shows the block diagram of a quadrature MZ. For the remainder of the paper, in block diagrams, we use single lines to represent electrical signals and double lines to represent optical signals.

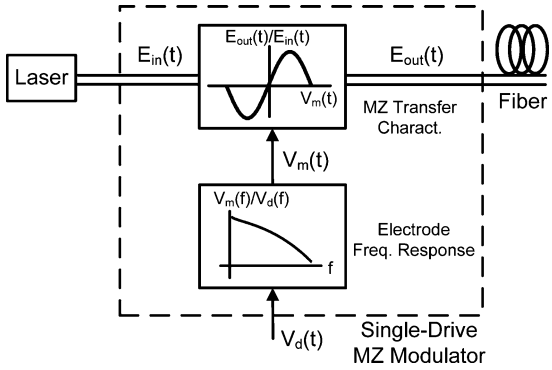

Fig. 1. Model for single-drive MZ modulator, corresponding to one phase of a quadrature MZ modulator.

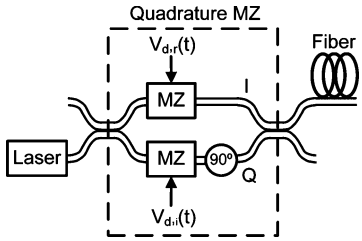

Fig. 2. Quadrature MZ modulator.

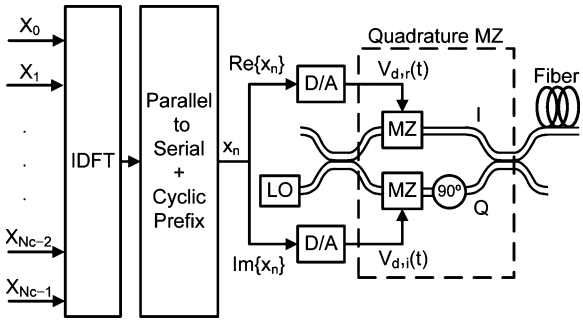

Fig. 3. OFDM transmitter using quadrature MZ modulator.

III. QUADRATURE MZ OPTIMIZATION

A. Quadrature MZ Modulator

Fig. 3 shows an optical OFDM modulator using a quadrature MZ.

In Fig. 3, the transmitted symbols are modulated using the inverse discrete Fourier transform (IDFT) and the cyclic prefix is added to the signal. After D/A conversion, the real and imaginary components are used to drive the MZ modulators. Then, one of the MZ outputs is delayed by 90° in order to generate the optical in-phase (I) and quadrature (Q) components. These are then summed and injected into the fiber. We note that in Fig. 3 not all the N_c subcarriers are used to transmit data. Some of the subcarriers are used for oversampling [2]. The oversampling ratio is defined as $M_s = N_c/N_u$ where N_c is the IDFT size and N_u is the number of used subcarriers [2]. Furthermore, the used

subcarriers are properly positioned within the DFT block such that the resulting OFDM spectrum is centered and, typically, the DC subcarrier is not used for data transmission.

The MZ modulators in Fig. 3 can introduce two impairments: low optical power efficiency and intermodulation products between subcarriers.

In order to quantify the first impairment, we define OPE as

$$\mathrm{OPE} = \frac{\text{Average Modulated Power}}{\text{CW Laser Power}}. \tag{6}$$

A backoff in the MZ operating range is required to accommodate the peak of any drive signal. Since the OFDM signals have a high PAR, the OPE can be very low. For example, if $N_c = 64$ and $M_s = 1.2$, i.e., 52 used subcarriers, the OPE is less than 1% (Fig. 8).

The second impairment results from the MZ nonlinear transfer characteristic. Expanding (4) into a Taylor series, we get

$$\frac{E_{\mathrm{out}}(t)}{E_{\mathrm{in}}(t)} = \sin\left(\frac{\pi V_m(t)}{2V_\pi}\right) \approx \frac{\pi V_m(t)}{2V_\pi} - \left(\frac{\pi V_m(t)}{2V_\pi}\right)^3 + \cdots. \tag{7}$$

The cubic term in (7) will generate in-band intermodulation products between the subcarriers, which cannot be removed by filtering.

In order to mitigate the previous impairments, we will use predistortion to compensate the MZ nonlinearity and hard clipping to increase the OPE. The clipping operation is described as

$$V_{\mathrm{in}}(n) = \begin{cases} -A, & \text{if } x(n) < -A \\ x(n), & \text{if } -A \le x(n) \le A \\ A, & \text{if } x(n) > A \end{cases} \tag{8}$$

where $V_{\mathrm{in}}(n)$ is the clipped signal at sample time n, and A is the clipping level. The clipping operation is done separately on each of the real and imaginary components of the OFDM signal. Furthermore, we will use a super-Gaussian filter (SGF) at the MZ output in order to eliminate any out of band leakage generated by hard clipping (in a practical wavelength division multiplexing (WDM) system, this filtering function would be performed by the multiplexer). The predistortion function is given by

$$V_{\mathrm{out}}(n) = \frac{2V_\pi}{\pi} \arcsin\left(\frac{V_{\mathrm{in}}(n)}{\max_n |V_{\mathrm{in}}(n)|}\right) \tag{9}$$

where $V_{\mathrm{in}}(n)$ and $V_{\mathrm{out}}(n)$ are the digital input and output voltages of the predistortion device. Note that $\max_n |V_{\mathrm{in}}(n)| = A$ because of the clipping operation and that the output signal $V_{\mathrm{out}}(n)$ swing is always between $-V_\pi$ and $+V_\pi$ due to the mapping of the predistortion curve. The predistortion transfer characteristic is shown in Fig. 4. In addition to the predistortion curve, we need to compensate the electrode frequency response of each MZ. We note that if the electrode frequency response is compensated, then $V_m(n) = V_{\mathrm{out}}(n)$. The optimized

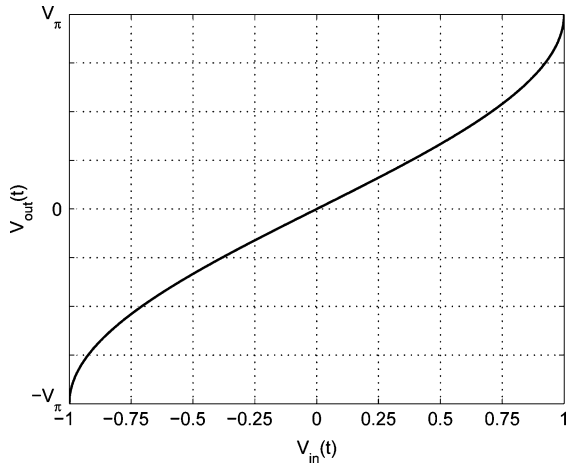

Fig. 4. Predistortion transfer characteristic for quadrature MZ modulator.

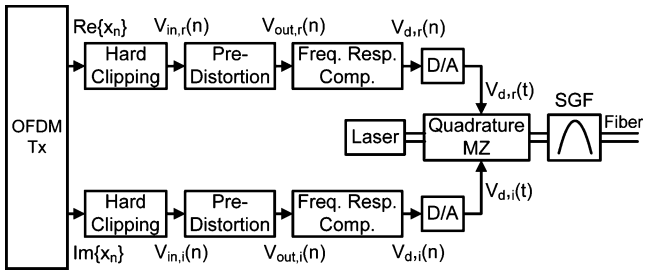

Fig. 5. OFDM transmitter including hard clipping, predistortion, and electrode frequency response compensation.

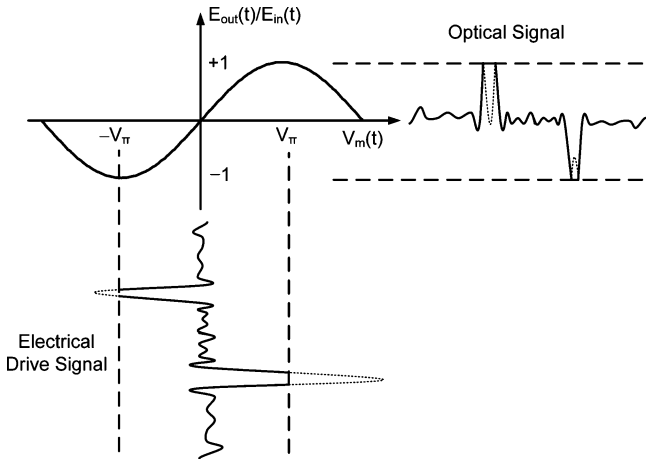

Fig. 6. Electrical and optical MZ waveforms. The solid and dotted lines represent the waveforms with and without hard clipping, respectively.

OFDM transmitter and the corresponding waveforms are shown in Figs. 5 and 6. In Fig. 5, we note that the peak after the D/A can exceed the value limited by the digital hard clipping device because of interpolation effects [10], [13]. In order to avoid an analog clipping device, we will allow the driving signal to exceed V_π. Later, we will show that this effect has negligible impact on system performance.

B. Clipping Simulation Results

In order to make the simulation results independent of the number of subcarriers, we will define a normalized clipping level called the clipping ratio (CR) [14], which is defined as

$$\mathrm{CR} = \frac{A}{\sigma} \tag{10}$$

where A is the clipping level and σ is the rms power of the OFDM signal, i.e., $\sigma = \sqrt{E[|x(t)|^2]}$. For example, if there is no clipping, then $\mathrm{CR} = \sqrt{\mathrm{PAR}}$. A value $\mathrm{CR} = 2$ means that the signal is clipped at twice the rms power level. We note that the PAR of the real and imaginary components is twice the PAR of the complex baseband OFDM signal, since the real and imaginary parts have half the power but the same peak value as the complex baseband OFDM signal.

In our simulations, we consider a polarization-multiplexed system with a total bit rate of 118 Gbit/s (103 Gbit/s with 15% FEC overhead). The subcarriers are modulated using QPSK, so the symbol rate on each polarization is 29.66 GHz. The FFT size is 64 and the oversampling ratio is $M_s = 1.2$, i.e., only 52 subcarriers are used. The cyclic prefix is chosen accordingly to [2], and is approximately 1/10 of the total number of subcarriers. We assume for now that the D/A has an infinite number of bits. We neglect all transmission impairments, such as fiber nonlinearity, GVD and PMD. We use a homodyne receiver, followed by an anti-aliasing filter that is a fifth-order Butterworth low-pass filter having a 3-dB bandwidth equal to 17.2 GHz, the first null in the baseband OFDM spectrum [2]. The 3-dB bandwidth of the SGF is set equal to the OFDM bandwidth [2]. The MZ 3-dB bandwidth is 30 GHz, which is representative of currently available devices [15]. The MZ frequency response is shown in Fig. 7. We note that the compensation of the MZ frequency response shown in Fig. 5 requires one extra DFT and IDFT operation to scale the subcarriers by the inverse of the MZ electrode frequency response. We consider three scenarios for the modulator: *FullCompensation* where we compensate the MZ electrode frequency response as shown in Fig. 5, *Precompensation* where we move the electrode frequency response compensation to the OFDM transmitter as a predistortion operation, i.e., we are swapping the order of the nonlinear and linear effects and *NoCompensation* where we do not compensate the MZ electrode frequency response. The simulation results are shown in Figs. 8 and 9. Since typical current FEC codes have a threshold around $P_S = 10^{-3}$, we measure the receiver sensitivity penalty at $P_S = 10^{-4}$ in order to have some margin.

In Fig. 8, we observe that the OPE is around 1% if there is no clipping ($\mathrm{CR} = 10.2$). As we start clipping, the power efficiency increases significantly. Moreover, we can also observe that the three compensation options have approximately the same OPE. For the case of no compensation, the OPE is slightly inferior, due to the frequency dependence of the MZ electrode frequency response.

In Fig. 9, we observe that the power penalty is approximately constant down to about $\mathrm{CR} = 2.5$, below which, the signal becomes severely distorted and the receiver sensitivity penalty increases rapidly. Furthermore, we observe that the three compensation scenarios have approximately the same performance. For the case of no compensation, we note that there is a residual receiver sensitivity penalty even if there is no clipping. The residual receiver sensitivity penalty is due to the power lost at

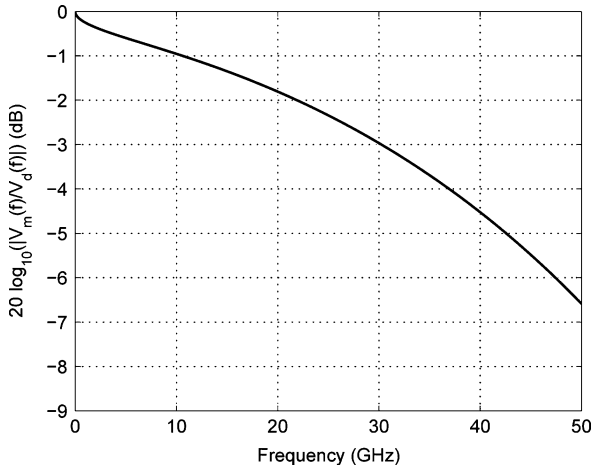

Fig. 7. MZ electrode frequency response.

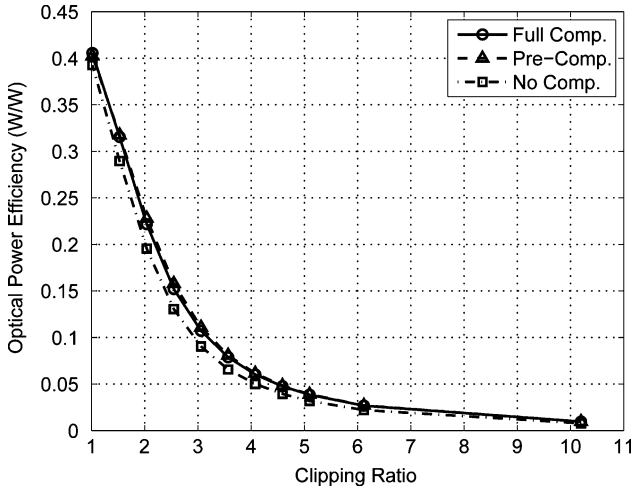

Fig. 8. Optical power efficiency for $N_c = 64$, $N_u = 52$, and $R = 29.66\,\mathrm{GHz}$.

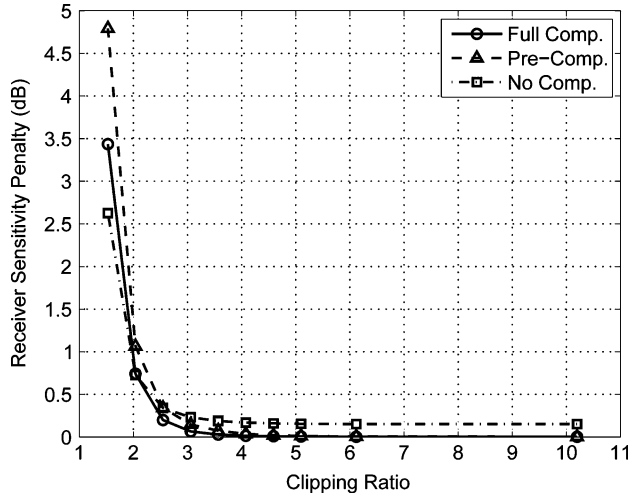

Fig. 9. Receiver sensitivity penalty at $P_S = 10^{-4}$, $N_c = 64$, $N_u = 52$, and $R = 29.66\,\mathrm{GHz}$.

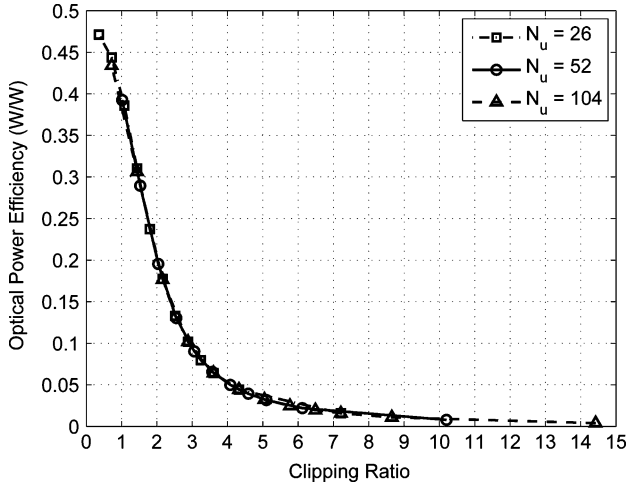

Fig. 10. Optical power efficiency for different number of subcarriers.

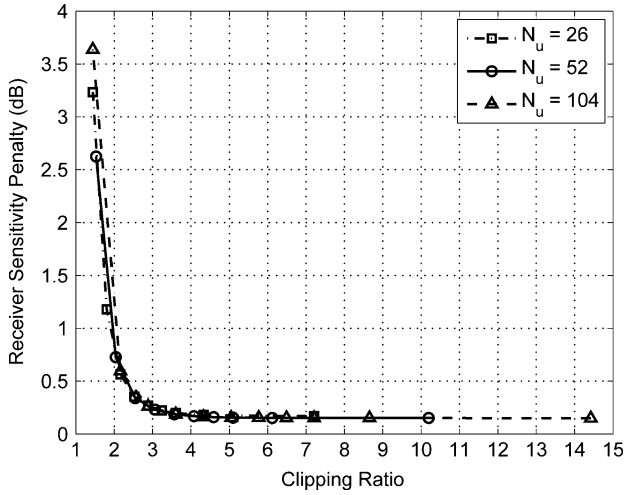

Fig. 11. Receiver sensitivity penalty for different number of subcarriers.

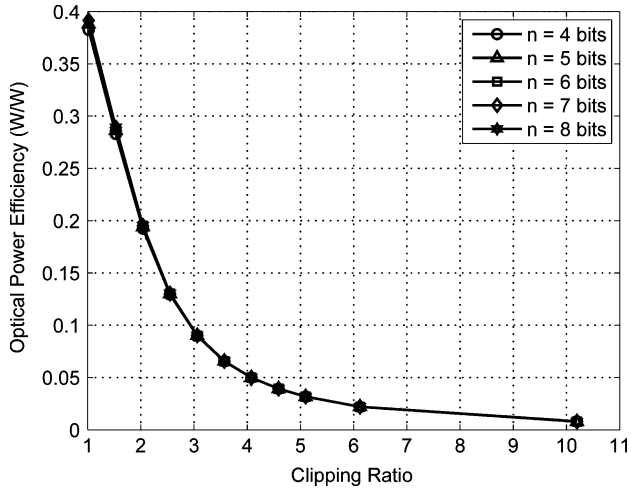

Fig. 12. Optical power efficiency for different number of bits in the D/A, $N_c = 64$, $N_u = 52$, and $R = 29.66\,\mathrm{GHz}$.

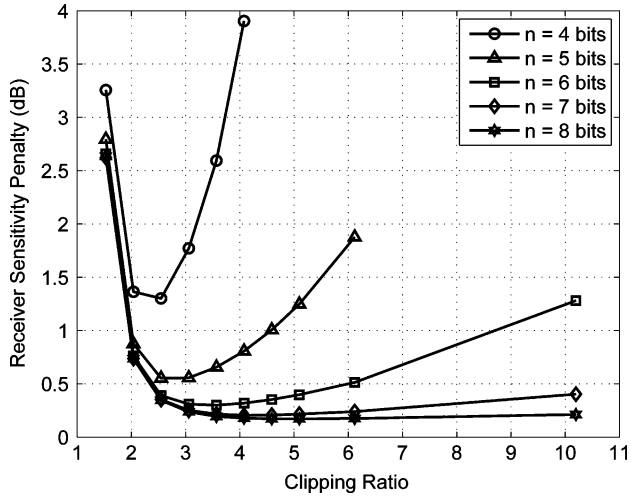

Fig. 13. Receiver sensitivity penalty for different number of bits in the D/A, $N_c = 64$, $N_u = 52$, and $R = 29.66\,\mathrm{GHz}$.

some frequencies in the MZ. By going from $\mathrm{CR} = 10.2$ (no clipping) down to $\mathrm{CR} = 2.5$, the OPE increases from less than 1% to 14%, a 12-dB power gain at the cost of a 0.5-dB sensitivity penalty.

Finally, in order to confirm that the CR makes the optimized clipping level independent of the number of subcarriers, we repeated the simulations with a different number of subcarriers. Figs. 10 and 11 show the OPE and system performance curves for different numbers of subcarriers for the case of no compensation of the MZ electrode frequency response.

C. Quantization Effects

For the remainder of the paper, we consider only the situation where the electrode frequency response is not compensated, since we verified that this compensation has little effect on OPE and system performance. In addition, not compensating the electrode frequency response minimizes hardware complexity and power consumption.

In a practical OFDM transmitter, the D/A necessarily will have a finite number of bits. Figs. 12 and 13 show the OPE and system performance curves for different number of bits in the D/A. We note that the D/A reference voltage is always equal to V_π regardless of the CR, since the predistortion device maps the clipped peak value to $\pm V_\pi$.

In Fig. 12, we observe that the OPE is independent of the number of bits in the D/A. On the other hand, in Fig. 13 we observe that for a fixed number of bits, the receiver sensitivity penalty decreases as we further clip the signal until around $\mathrm{CR} = 2.5$. This is because the D/A with a limited number of quantization levels can better represent the OFDM signal as the peak is further clipped. We also observe that as we increase the number of bits, the receiver sensitivity penalty decreases and converges to the case of infinite-resolution value, as expected. If a value $\mathrm{CR} = 2.5$ is used, 6 bits would be sufficient to obtain good performance. Finally, we note that although we considered $N_u = 52$ in Figs. 12 and 13, the receiver sensitivity penalty due to clipping and quantization is independent of the number of subcarriers for a given value of CR.

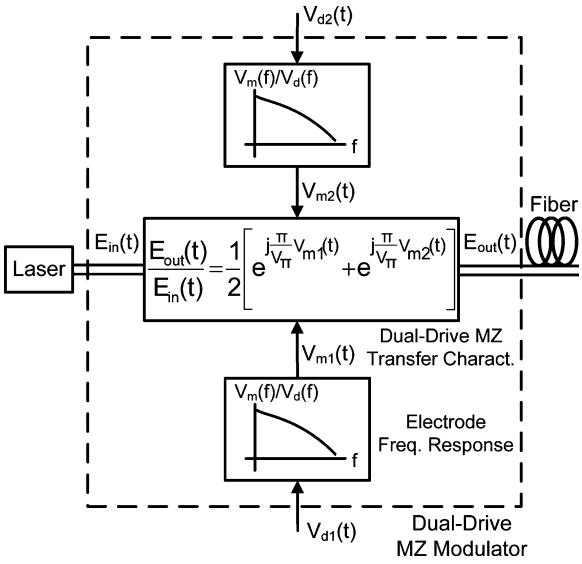

Fig. 14. Model for dual-drive MZ modulator.

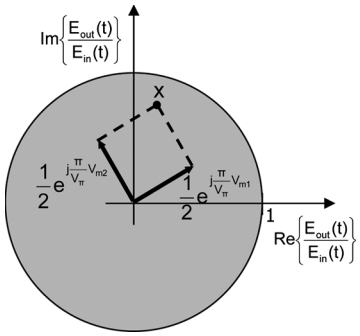

Fig. 15. Dual-drive MZ plane.

IV. Dual-Drive MZ Optimization

A. Dual-Drive MZ Modulator

We have shown that the quadrature MZ can be used as an efficient OFDM transmitter. In an attempt to reduce complexity, we have also considered using a dual-drive MZ as an OFDM transmitter. The dual-drive MZ has two independent drive electrodes, and has transfer characteristic given by

$$\frac{E_{\text{out}}(t)}{E_{\text{in}}(t)} = \frac{1}{2}\left[e^{j\pi/V_\pi V_{m1}(t)} + e^{j\pi/V_\pi V_{m2}(t)}\right] \qquad (11)$$

where $E_{\text{out}}(t)$ and $E_{\text{in}}(t)$ are the output and input electric fields, respectively, $V_{m1}(t)$ and $V_{m2}(t)$ are independent electrical modulator signals and V_π is the drive voltage that must be applied differentially between the two electrodes to produce a differential phase shift of π between the two waveguides. The model for the dual-drive MZ is shown in Fig. 14.

The frequency response of each electrode in Fig. 14 is given by (5). In the dual-drive MZ, by adding together two independent signals whose phases are proportional to the two independent drive voltages, we can generate an output electric field having arbitrary magnitude and phase. In other words, we can generate any point inside the unit circle of the complex plane $E_{\text{out}}(t)/E_{\text{in}}(t)$, as shown in Fig. 15.

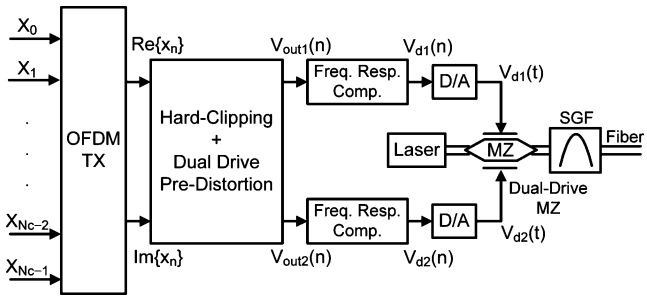

Fig. 16. OFDM transmitter using the dual-drive MZ with hard-clipping, predistortion, and electrode frequency response compensation.

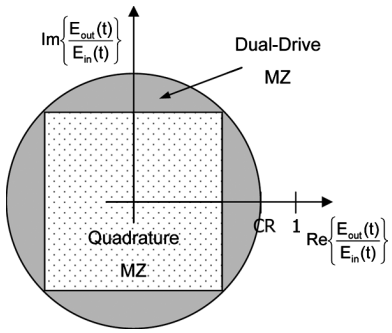

Fig. 17. OFDM span regions for a fixed clipping level. The dotted and solid regions correspond to the quadrature MZ and the dual-drive MZ, respectively.

The drive voltages required to generate a point $x = Ae^{j\theta} (0 \leq A \leq 1)$ are given by

$$V_{\text{out1}} = \frac{V_\pi}{\pi}(\theta + \arccos(A) + 2\pi q)$$

$$V_{\text{out2}} = \frac{V_\pi}{\pi}(\theta - \arccos(A) + 2\pi q). \qquad (12)$$

We note that due to the symmetry of the problem, the equations for V_{out1} and V_{out2} are periodic with period $2V_\pi$ and that they could be interchanged and the point x would still be obtained. We note that if the frequency response of each electrode is compensated, then $V_{m1}(n) = V_{\text{out1}}(n)$ and $V_{m2}(n) = V_{\text{out2}}(n)$.

As for the quadrature MZ modulator, we use hard clipping in the dual-drive MZ to increase the OPE. The optimized OFDM transmitter using the dual-drive MZ is shown in Fig. 16.

Besides reduced hardware complexity, another advantage of the dual-drive MZ over the quadrature MZ is a reduced clipping probability for the same clipping level. As shown in Fig. 17, the dual-drive MZ can span the indicated circle in the complex plane $E_{\text{out}}(t)/E_{\text{in}}(t)$ for a given clipping level, while the quadrature MZ can only span the indicated square.

If the drive signal samples $V_{m1}(n)$ and $V_{m2}(n)$ are digitally predistorted, the MZ will generate the correct optical electric field at the sampling instants. However, the drive voltages $V_{m1}(t)$ and $V_{m2}(t)$ between samples are obtained by interpolation in the D/A converter, and they are not generally the values required to generate the correct optical electric field in between the sampling instants. As shown in Fig. 18, the optical waveform will differ from the correct OFDM waveform, which can

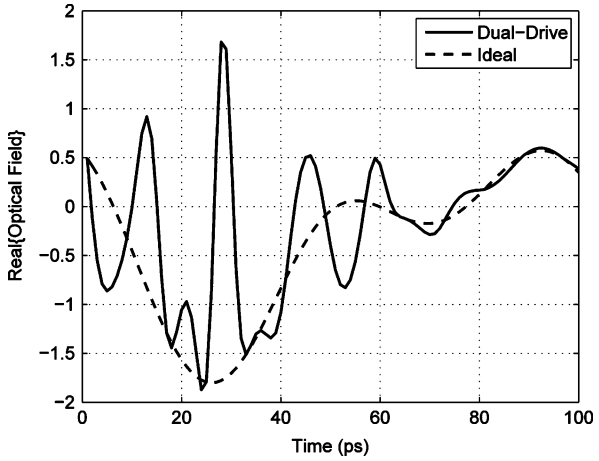

Fig. 18. Real component of the dual-drive MZ output electric field.

degrade system performance. This problem can be controlled by increasing the oversampling ratio.

However, for a fixed oversampling ratio, there are some degrees of freedom in selecting the drive voltage values at the sampling instants since the dual-drive nonlinear transfer characteristic is periodic with period $2V_\pi$ and drive voltage values for V_{m1} and V_{m2} can be interchanged. The correct OFDM values in between the sampling instants are obtained by smooth interpolation (ideally $\mathrm{sinc}()$ interpolation). So, in order to minimize the error in between the sampling instances, the trajectory spanned by the drive voltage vectors in the complex plane $E_{\mathrm{out}}(t)/E_{\mathrm{in}}(t)$ should also be smooth, which is analogous to

$$\begin{aligned} &\text{minimize} \quad |\Delta V_{m1}(r)| + |\Delta V_{m2}(r)| \\ &\quad \text{subject to} \quad V_{m1}(n) = V_{\mathrm{out}i}(n), \quad n = r, r+1 \end{aligned} \tag{13}$$

where $|\Delta V_{mi}(r)| = |V_{mi}(r) - V_{mi}(r+1)|$ and $i = 1, 2$. In (13), we note that once the predistortion equation for $V_{m1}(n)$ is chosen, the equation for $V_{m2}(n)$ is constrained such that the optical electrical field at the sampling instant is equal to the OFDM sample value.

Fig. 19 illustrates the output optical electrical field generated by the dual-drive MZ for the cases of no trajectory optimization and with trajectory optimization for an oversampling ratio of $M_s = 2.5$ before the SGF.

In Fig. 19(a), no trajectory optimization was used and the drive voltages were set to $V_{m1}(n) = V_{\mathrm{out}1}(n)$ and $V_{m2}(n) = V_{\mathrm{out}2}(n)$ for all discrete time n and they were limited to the range between $-V_\pi$ to $+V_\pi$. We observe that the optical field in between the sampling instants is not equal to the correct OFDM waveform for the majority of the time. However, in Fig. 19(b), we observe that the error in between the sampling instants is significantly minimized when trajectory optimization is used. The receiver sensitivity penalty is around 1 dB for an oversampling ratio $M_s = 2.5$ when trajectory optimization is used. On the other hand, if no trajectory optimization is used, the oversampling ratio to achieve 1-dB receiver sensitivity penalty is $M_s \geq 5$. Finally, in Fig. 19(c), we have expanded the drive voltages range to $\pm 2V_\pi$ and the error in between samples was further reduced since there are now more degrees of freedom for the drive voltages values. The receiver sensitivity penalty

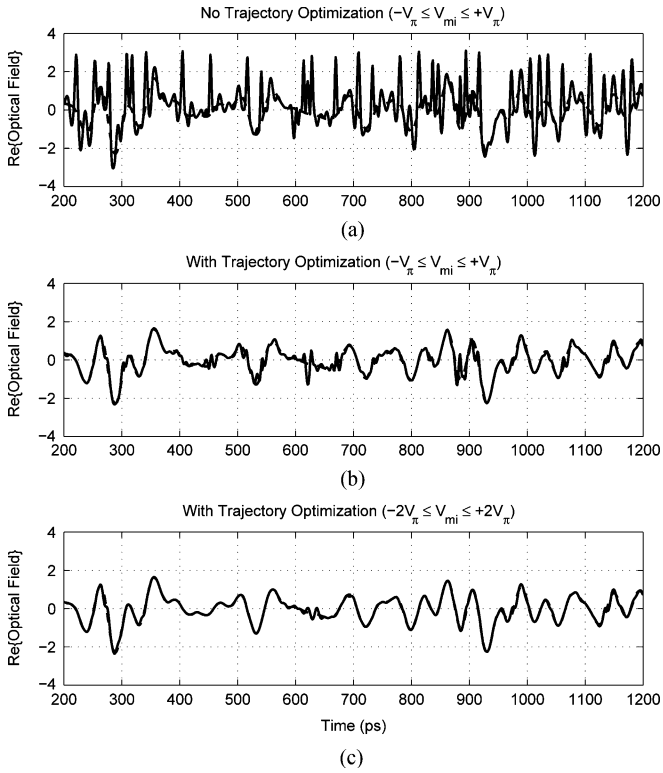

Fig. 19. Output electric field of the dual-drive MZ for the cases of no trajectory optimization and with trajectory optimization before the SGF. The solid and dashed lines represent the output electric field and the correct OFDM waveform, respectively.

for this case is around 0.7 dB. We note that increasing the drive voltage range by a factor of two reduces the effective vertical resolution of the D/A converter by the same factor which, in turn, means that a larger number of bits is required to maintain the same performance. However, we believe that in a practical MZ modulator, the drive voltages values will be constrained to $\pm V_\pi$, so we will only consider this case for the remainder of the paper. Figs. 20 and 21 show the dual-drive MZ optical power efficiency and receiver sensitivity penalty, respectively, for different clipping levels.

We observe in Fig. 20 that the OPE increases significantly as we further clip the signal, like in the quadrature MZ. In Fig. 21, we notice that the power penalty is approximately constant down to about $\mathrm{CR} = 2.5$, below which, the signal becomes severely distorted and the receiver sensitivity penalty increases rapidly. Finally, from Figs. 20 and 21, we conclude that the optimum clipping level is $\mathrm{CR} = 2.5$, as for the quadrature MZ.

In Fig. 22, we compare the receiver sensitivity penalty for the two types of modulators as a function of the oversampling ratio at the optimum clipping level, $\mathrm{CR} = 2.5$.

We observe in Fig. 22 that the quadrature MZ penalty remains constant as we increase the oversampling ratio. The 0.4 dB residual penalty can be decomposed into 0.15 dB from the MZ frequency-dependent electrode losses and 0.25 dB from the clipping noise. On the other hand, the dual-drive MZ penalty decreases as the oversampling ratio increases. This is expected, as increasing the number of sampling points reduces the error between the correct and attainable waveform trajectories in the

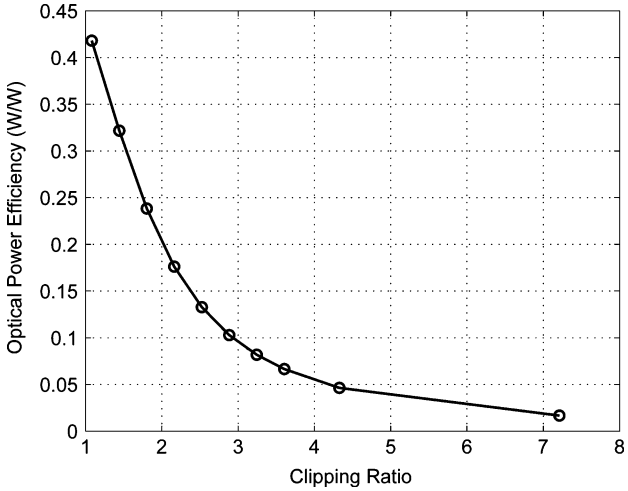

Fig. 20. Dual-drive MZ optical power efficiency with trajectory optimization for $M_s = 2.5$, $N_u = 52$, and $R = 29.66\,\mathrm{GHz}$.

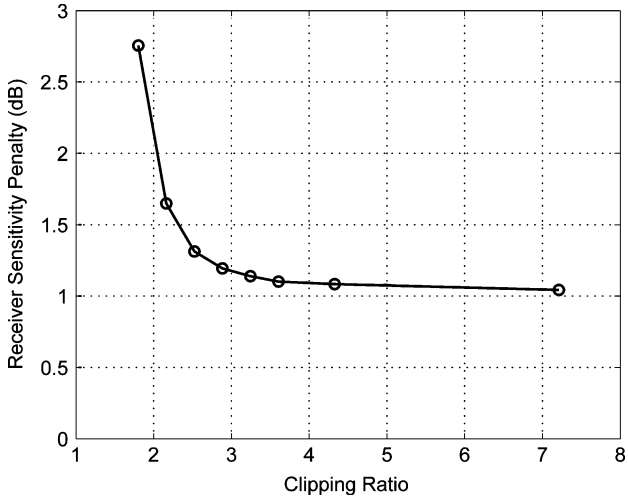

Fig. 21. Dual-drive MZ receiver sensitivity penalty with trajectory optimization for $M_s = 2.5$, $N_u = 52$, and $R = 29.66\,\mathrm{GHz}$.

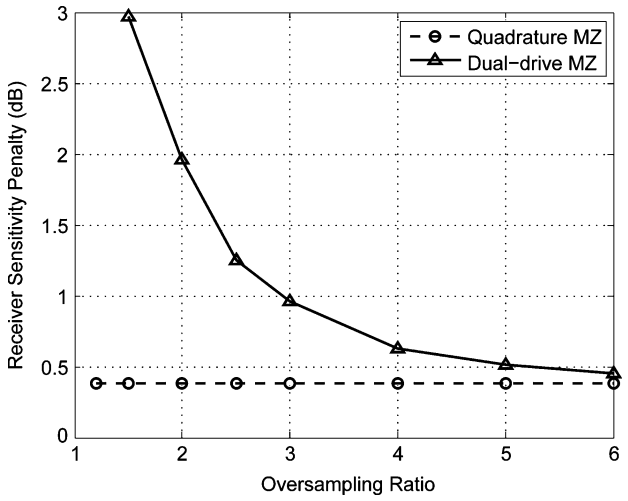

Fig. 22. Dual-drive and quadrature MZ receiver sensitivity penalties as a function of the oversampling ratio with no frequency loss compensation and with trajectory optimization for $\mathrm{CR} = 2.5$, drive voltages range between $\pm V_\pi$ and $R = 29.66\,\mathrm{GHz}$.

complex plane. Finally, we note that the dual-drive receiver sensitivity penalty converges to the same value as that for the quadrature MZ as the oversampling ratio increases.

V. Conclusion

We have shown that the quadrature MZ with predistortion and hard clipping is able to achieve good performance without additional oversampling, while achieving high optical power efficiency. We observed that the MZ electrode frequency-dependent losses can be neglected, since they have very little impact on system performance. We have also shown that the optimum clipping level is approximately $\mathrm{CR} = 2.5$, since this value yields a 12-dB gain in optical power efficiency with minimal receiver sensitivity degradation. Furthermore, we verified that the D/A requires at least 6 bits, and that the optimum clipping level is also approximately $\mathrm{CR} = 2.5$ when quantization noise is present. We have also shown that the dual-drive MZ can also be used as an efficient OFDM modulator. It requires less hardware than the quadrature MZ and minimizes the clipping probability. On the other hand, the dual-drive MZ requires a higher oversampling ratio which, in turn, means that faster D/A converters and wider electrode frequency responses are necessary.

Acknowledgment

The authors would like to thank Alan P. T. Lau and Ezra Ip for helpful discussions and suggestions.

References

[1] S. Jansen, I. Morita, T. Schenk, N. Takeda, and H. Tanaka, "Coherent optical 25.8-Gb/s OFDM transmission over 4160-km SSMF," *J. Lightw. Technol.*, vol. 26, no. 1, pp. 6–15, Jan. 2008.

[2] D. J. F. Barros and J. M. Kahn, "Optimized dispersion compensation using orthogonal frequency-division multiplexing," *J. Lightw. Technol.*, vol. 26, no. 16, pp. 2889–2898, Apr. 2008.

[3] G. L. Stüber, *Principles of Mobile Communication*, 2nd ed. Boston, MA: Kluwer Academic, 2001.

[4] B. J. C. Schmidt, A. J. Lowery, and J. Armstrong, "Experimental demonstrations of 20 Gbit/s direct-detection optical OFDM and 12 Gbit/s with a colorless transmitter," in *Proc. OFC'07*, 2007, postdeadline paper PDP18.

[5] Y. Tang, W. Shieh, X. Yi, and R. Evans, "Optimum design for RF-to-Optical up-converter in coherent optical OFDM systems," *IEEE Photon. Technol. Lett.*, vol. 19, no. 7, pp. 483–485, Apr. 2007.

[6] Y. Tang, K. Ho, and W. Shieh, "Coherent optical OFDM transmitter design employing predistortion," *IEEE Photon. Technol. Lett.*, vol. 20, no. 11, pp. 954–956, Jun. 2008.

[7] B. Krongold and D. Jones, "PAR reduction in OFDM via active constellation extension," *IEEE Trans. Broadcast.*, vol. 49, no. 3, pp. 258–268, Sep. 2003.

[8] S. Sezginer and H. Sari, "OFDM peak power reduction with simple amplitude predistortion," *IEEE Commun. Lett.*, vol. 10, no. 2, pp. 65–67, Feb. 2006.

[9] C. Ciochina, F. Buda, and H. Sari, "An analysis of OFDM peak power reduction techniques for WiMAX systems," in *Proc. IEEE ICC'06*, 2006, vol. 10, pp. 4676–4681.

[10] J. Tellado, *Multicarrier Modulation with Low PAR: Applications to DSL and Wireless*. Boston: Kluwer Academic, 2000.

[11] A. J. Lowery, S. Wang, and M. Premaratne, "Calculation of power limit due to fiber nonlinearity in optical OFDM systems," *Opt. Express*, vol. 15, no. 20, pp. 13282–13287, 2007.

[12] K. P. Ho, *Phase-Modulated Optical Communication Systems*. New York: Springer, 2005.

[13] J. Armstrong, "Peak-to-average power reduction for OFDM by repeated clipping and frequency domain filtering," *Electron. Lett.*, vol. 38, no. 5, pp. 246–247, Feb. 2002.

[14] X. Li and J. L. J. Cimini, "Effects of clipping and filtering on the performance of OFDM," *IEEE Trans. Veh. Technol.*, vol. 3, 1997, **[PLEASE PROVIDE MONTH, AND ISSUE AND PAGE NUMBERS**.

[15] 40 Gbps $LiNbO_3$ External Modu. 2004 [Online]. Available: http://www.fujitsu.com/global/services/telecom/optcompo/lineup/40gln/

Daniel J. Fernandes Barros received the Licenciatura degree (with honors) in electrical and electronics engineering from the University of Porto, Portugal, in 2004, and the M.S. degree in electrical engineering from Stanford University, Stanford, CA, in 2007, where he is currently working toward the Ph.D. degree in electrical engineering.

His current research interests include single-mode optical-fiber communication, digital signal processing, and RF circuits.

Joseph M. Kahn (M'90–SM'98–F'00) received the A.B., M.A., and Ph.D. degrees in physics from the University of California, Berkeley, in 1981, 1983, and 1986, respectively.

From 1987 to 1990, he was with AT&T Bell Laboratories, Crawford Hill Laboratory, Holmdel, NJ. He demonstrated multigigabits-per-second coherent optical-fiber transmission systems, setting world records for receiver sensitivity. From 1990 to 2003, he was a faculty member with the Department of Electrical Engineering and Computer Sciences, University of California, Berkeley, where he was engaged in research on optical and wireless communications. In 2000, he helped found StrataLight Communications, where he was a Chief Scientist from 2000 to 2003. Since 2003, he has been a Professor of electrical engineering with Stanford University, Stanford, CA. His current research interests include single and multimode optical-fiber communications, free-space optical communications, and microelectromechanical systems for optical communications.

Prof. Kahn was the recipient of the National Science Foundation Presidential Young Investigator Award, in 1991. From 1993 to 2000, he was a Technical Editor of *IEEE Personal Communications Magazine*.